

LASER TRANSFER DOPING USING AMORPHOUS SILICON

Rafel Ferré (*Correspondence author*)¹, Ralf Gogolin¹, Jens Müller¹, Nils-Peter Harder^{1,2}, Michael Kessler¹, Christoph Mader¹, Peter Giesel¹, Tobias Neubert¹, Rolf Brendel^{1,3}

¹Institute for Solar Energy Research Hamelin (ISFH), Am Ohrberg 1, 31860 Emmerthal, Germany.

²Institut für Materialien und Bauelemente der Elektronik, Universität Hannover, Schneiderberg 32, 30167 Hannover, Germany

³Institute of Solid-State Physics, University of Hannover, Appelstrasse 2, 30167 Hannover, Germany
Tel +49(0)5151 999 413, Fax: +49 (0)5151 999 400, e-mail: ferre@isfh.de

ABSTRACT: We demonstrate and characterize “Laser Transfer Doping” (LTD) for producing locally doped regions. For this purpose we use nanosecond pulsed laser for transferring phosphorus doped amorphous silicon from a carrier glass to silicon wafers. The phosphorus is transferred into the silicon wafer substrate and produces local doping. We use this process to produce local high-low junctions for the formation of n^+-n Back or Front Surface Fields that are directly contacted with aluminum. We find low surface recombination velocities and low contact resistance when transferring layers through a thin (13 nm) thermally grown silicon oxide. We also apply this process for contacting the phosphorus-doped front surface field of n-type rear junction solar cells. With this contact system we achieve open circuit voltages above 670 mV and fill factors close to 80%. The best solar cell efficiency in these initial investigation reaches 19.4% with open-circuit voltage of 664 mV and fill factor of 75.6%.

1 INTRODUCTION

In homojunction high efficiency silicon solar cells highly-doped regions are prepared under the contacts of the rear side to reduce series resistance and perform field-effect passivation. Traditional ways to produce these structures require deposition and selective etching of a barrier, diffusion of doping elements and eventually removal of the barrier. For p-type contacts Laser Fired Contacts (LFC) [1] are a convenient solution to simplify the process: The LFC process provides the perforation of the passivation layer and Al-doping at the contact area in one step, but not to the same high quality as achievable by furnace diffusion of dopants. For n-type contacts Suwito et al. recently presented the PassDop process [2], where a phosphorus-containing passivation layer on a cell is employed for producing n^+ -type regions. While the traditional method of diffusion barriers is cumbersome, both the LFC and the PassDop process require certain layers to be present on the actual cell structure. This might be a disadvantage for some applications. An alternative is to use Laser Transfer Doping (LTD) as sketched in the Fig. 1. This concept uses a laser to transfer a doped layer that is deposited on a glass substrate to the wafer.

Laser Transfer Doping was demonstrated using phosphor nitride as a doping source [3, 4]. From Ref [3] it is thus already known that LTD is technically feasible. However, the electronic quality in terms of carrier lifetime degradation and contact resistance has not been explored and shall be investigated and evaluated on solar cells in this present paper. Low recombination activity and low contact resistances are crucial for the applicability of LTD to solar cell processing. We use the LTD process to treat the contact regions of the solar cell and therefore the Si surface in between the laser transferred doped regions should be well passivated.

Recently we have demonstrated Laser Transfer Doping through a passivating dielectric layer [5]. We use laser pulses to transfer doped amorphous silicon from a transparent substrate to a wafer. In this paper we review the characteristics of the LTD process for laser-transferring phosphorus-doped a-Si through a silicon oxide passivation layer on a planar silicon wafer surface

as may be applicable to the rear side of n-type PERL-Solar cells. We also report the results of initial solar cell experiments that explore the LTD process for preparing the heavily doped regions in a (metal contacted) selective front-surface field (FSF) of n-type back-junction solar cells. In this case, we perform the LTD process through a passivating SiN layer on a textured surface

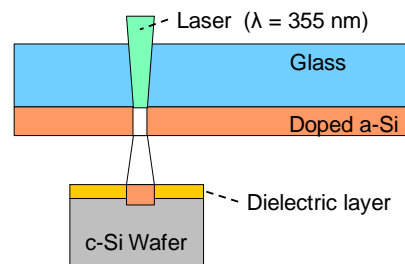


Figure 1: Schematic of the Laser Transfer Doping process.

2 RECOMBINATION UNDER LTD REGIONS

As substrate for the a-Si layer we use borosilicate glass with a thickness of 1.1 mm. We deposit on it 300 nm of phosphorus-doped a-Si by Plasma Enhanced Chemical Vapor Deposition (PECVD). For investigating the general characteristics of the LTD process we use two different contact systems:

2.1 Rear-side passivation scheme with SiO₂

We use planar, (100) oriented n-type Float Zone silicon wafers, with a resistivity around 2 Ω cm. We perform a dry thermal oxidation producing a 13 nm thick silicon oxide (SiO₂). Afterwards we position the glass on the wafer with the a-Si coated side facing the wafer and perform the LTD process as is shown schematically in Figure 1.

We produce square patterns of single laser pulses using a nanosecond laser working at a wavelength of 355 nm. We vary the energy of the laser pulse from 12 to 121 μJ and the pitch (distance between two spots) from 200 to 600 μm. The laser spot size on the wafer ranges from 50 to 120 μm. After the LTD process, half of the samples

receive an annealing step at 900°C for 30 min in Nitrogen atmosphere. We improve the passivation of the front side by depositing 100 nm PECVD-SiN onto the 13nm thermally grown SiO₂. Then, we evaporate a layer of 5 μm Aluminum onto the rear side, followed by annealing at 400 °C for 15 min. This “anneal” process leads to hydrogenation of the SiO₂-Si interface and good surface passivation. The final surface recombination velocity is determined in reference samples without LTD process and coated symmetrically with the corresponding SiO₂/SiN and SiO₂/Al structures, respectively.

2.2 Selective Front Surface Field (FSF) scheme with SiN

We use pyramidal textured, (111) oriented, n-type Cz silicon wafers with a resistivity around 2 Ω cm. We perform a 200 to 500 Ω/sq phosphor diffusion. We passivate the surface with a passivation silicon nitride (SiN_{n=2.4}, 15 nm thick, refractive index at 632 nm n=2.4). Then we perform the LTD process as described above. Finally we produce a silicon nitride antireflection coating (SiN_{n=2.05}, 80 nm, n=2.05). We also produce reference samples without LTD to determine the surface recombination velocity at the passivated regions.

2.3 Surface Recombination Velocity

We use the approach of Müller et al [6] based on the analytical model of Fischer [7] to describe the area-averaged effective rear recombination velocity $S_{\text{eff, rear}}$ as a function of the contact recombination velocity $S_{\text{eff, cont}}$ and the metallization fraction f . To this end we use dynamically calibrated steady-state ILM measurements to experimentally evaluate $S_{\text{eff, rear}}$. We additionally use an optical microscope, prior to the actual aluminum evaporation, to determine the metallization fraction as a function of the radius r and the contact pitch p . The $S_{\text{eff, cont}}$ can then be extracted as explained in [2]. The corresponding values are plotted in Figure 2 as a function of the laser energy.

We obtain $S_{\text{eff, cont}}$ values between 20 and 100 cm/s for the SiO₂ coated samples that received a 900°C furnace anneal after the LTD process. The same kind of samples without such annealing produced S -values of 500 and 1500 cm s⁻¹ in the LTD-treated area. Measurement of the references without LTD processing indicate that the SiO₂/Al passivated regions has a surface recombination velocity of 7 ± 1 cm s⁻¹.

For the SiN samples we obtain values of $S_{\text{eff, cont}}$ between 200 and 500 cm s⁻¹ in the LTD-treated regions, while the corresponding SiN-passivated reference without LTD treatment showed surface recombination values of 10 ± 2 cm s⁻¹. The SiN coated samples were LTD-processed with lower laser energy than the oxide-passivated samples; however, the $S_{\text{eff, cont}}$ values of both types of samples seems to follow the identical trend as a function of the laser energy.

3 CONTACT RESISTANCE

For the SiO₂ samples we measure current-voltage I - V characteristics of samples that received the LTD process and metallization on both sides. All characteristics show an ohmic behavior, except for LTD-processed samples with the lowest laser energy if they additionally received the 900°C annealing. In this case the voltage dependence of the I - V characteristics slightly deviates from a linear behavior. We discard these samples for the following analysis. We follow the approach of Brooks and Mattes

[8] to estimate the effective resistance of the wafer.

Figure 3 plots the calculated series resistance as a function of the laser energy. The contact resistance reduces from 300 to 1 mΩ cm² when the energy increases from 20 to 120 μJ and is almost independent of the annealing conditions.

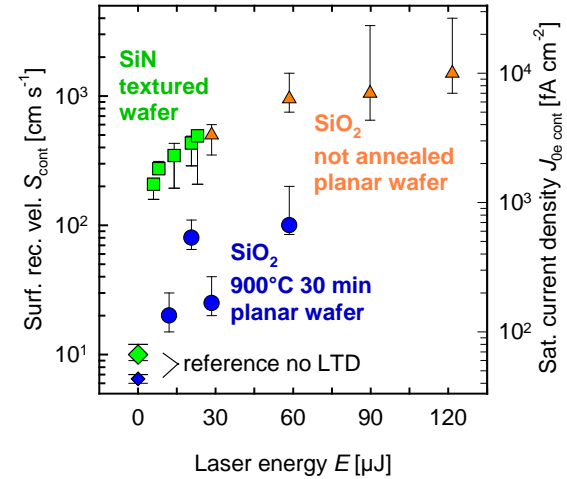


Figure 2: Contact surface recombination velocity S_{cont} as determined from the fit for 13 nm thermal silicon oxide (circles: annealed at 900°C, triangles: not-annealed) and for 15 nm SiN_{2n=2.4}/SiN_{n=2.05} (squares). Diamonds indicate the surface recombination velocity of the corresponding passivated regions (small/blue: SiO, big/green: SiN). Right axis gives the corresponding values for the saturation current densities as calculated from the S_{cont} -values.

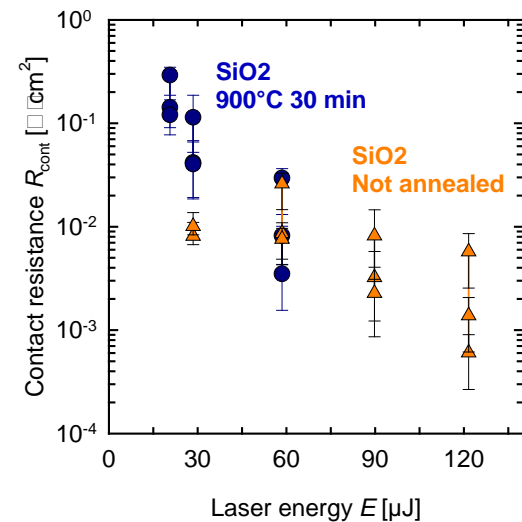


Figure 3: Contact resistance as a function of the laser energy through 13 nm thermal silicon oxide. Circles: annealed samples. Triangles: not annealed samples.

4 BACK-JUNCTION SOLAR CELLS

We prepare back-junction solar cells by using n-type wafers, 240 μm thick with a boron diffused rear emitter and a phosphorus-diffused textured front surface field. These back-junction solar cells are equipped with a rear metallization of evaporated aluminum for contacting the p-type rear emitter, and an evaporated Al contact grid at the front side for contacting the n-type FSF. In order to

optimize the contact resistance and contact recombination of the FSF, we treat the contact regions of the FSF with our LTD process. The solar cell structure is shown in Fig. 4 a) and the fabrication details are similar to those reported in [9]. In that previous work the front surface field is produced by a 80 Ohm/sq phosphorus diffusion, followed by Al evaporation through a shadow mask and afterwards a silicon nitride double layer to produce passivation (15 nm of $\text{SiN}_{n=2.4}$) and antireflection properties (80 nm of $\text{SiN}_{n=2.05}$.) For the solar cells of this previous work, the doping profile of the FSF had to be chosen as a compromise between (a) minimizing recombination in between the front metal fingers, and (b) minimizing recombination in the metalized regions under the metal fingers, combined with minimizing the contact resistance to the FSF. In between the fingers a shallow doping profile with low surface concentration is preferable, whilst underneath the metal fingers the opposite condition is favorable. We therefore use our LTD process for local doping in order to produce selective FSF structures that fulfill both conditions simultaneously: heavy doping in the metalized regions and light doping in the passivated regions.

We use full area FSF furnace diffusion with sheet resistance of 200 to 500 Ω/sq . In the passivated regions, this lightly doped FSF is beneficial due to reduced Auger recombination within this layer and low surface recombination velocity due to the lower surface doping density. The corresponding saturation current density with the double SiN layer passivation is $J_0 = 23 \text{ mA cm}^{-2}$. An additional advantage of such lightly-doped FSF is that it produces less free-carrier absorption.

We use our LTD technique for producing heavily doped regions that are suitable for metal contacts. We produce a set of samples, where we vary the laser energy from 6 to 60 μJ .

In the present work we apply the LTD process already after the deposition of the first passivation layer of the SiN double-layer stack, and prior to the metallization and prior to the thicker AR-overcoat of the SiN double-layer. That is, the processing sequence of the front side is:

1. FSF preparation
2. Deposition of thin passivation $\text{SiN}_{2.4}$ (15nm, $n=2.4$)
3. Local heavy doping by LTD process
4. Aligned Al grid evaporation through shadow mask
5. Deposition of $\text{SiN}_{2.05}$ antireflection overcoat layer (80nm, $n=2.05$)

Figure 4 b) shows the three different geometries of the LTD patterns that we used in our solar cells reported here. Also shown are two different grid metallization geometries. In our solar cells we combine the LTD pattern geometries and metallization geometries as shown in Figure 4 b), and which are labeled by “Overlapping”, “Crossed” and “Fine”.

- In the “Overlapping” configuration the whole metal grid and the LTD geometry coincide and have to be aligned to each other. In order to guarantee identical structures for the LTD pattern and the shadow mask for the aluminum evaporation, we do the following procedure: We prepare a shadow mask from a silicon wafer by laser-machining it by the same program and same laser system than used for the LTD process. Hence, the contact area, i.e. the overlapping region between LTD

and metal, coincides with the metal area and with the LTD area as long as precise shadow mask positioning can be ensured for the evaporation. For the present experiment the area fraction of LTD processed surface and metalized region is 14%, and they coincide with the contact area. Due to the rather thick laser-machined silicon shadow masks, smaller metallization area fractions are not possible.

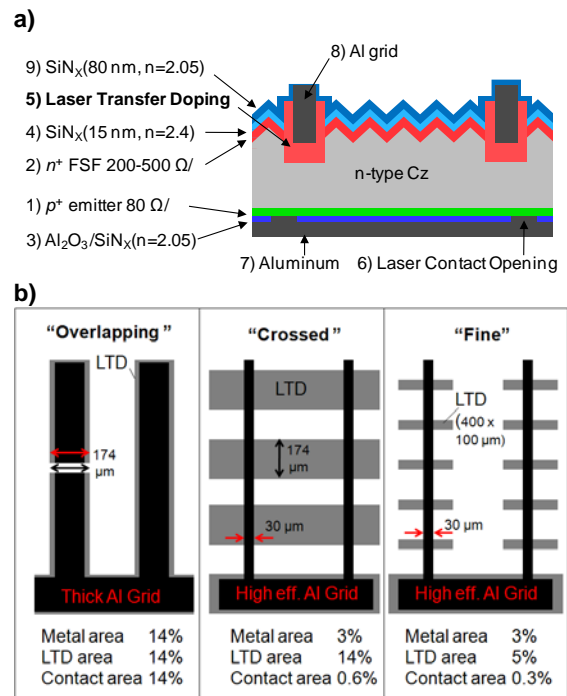


Figure 4: Application of Laser Transfer Doping to back-junction n-Wafer solar cells. a) Cross-view. The numbers indicate the process sequence. b) Designs of LTD and aluminum grid employed.

- The “Crossed” configuration as shown in Figure 4 b) uses the same area fraction (14%) for the LTD processed region. However, the geometry of the LTD region is different: LTD processed lines traverse the direction of the metal fingers by 90°. This configuration makes alignment obsolete and assures that any metallization mask (i.e. any finger width and finger-to-finger distance) will be able to establish contact to the solar cell. We use a thin metal mask that produces a narrow aluminum grid with 30 μm wide fingers and a total metal coverage of about 3% (Finger pitch of about 1mm). Due to the perpendicular configuration between the LTD-lines and the metal fingers, the actual semiconductor-metal contact area is only about 0.6%. Note that this configuration is similar to the “semiconductor fingers” structure as proposed by Mai [10].

- The configuration labeled as “Fine” in Figure 4 b) employs the same narrow aluminum grid as the “Crossed” configuration. However, in the “Fine” configuration, the LTD-processed area is reduced by making the LTD-“semiconductor fingers” much narrower (100 μm wide) and by interrupting them in between the later positions of the aluminum fingers. Thus we only apply the LTD process to a set of 400x100 μm^2 sized rectangles with a pitch of 600 μm . The length of 400 μm is

chosen to admit sufficient tolerance for the positioning of the shadow mask, i.e. of the metal fingers. As a result of this “Fine” configuration, the LTD is reduced to 5%, and the metal-semiconductor actual contact area is reduced to only 0.3%. The metallized area fraction is determined by the shadow mask geometry and thus remains at 3%, like in the “Crossed” configuration.

We also prepare two additional structures without LTD process. The first structures are samples with the aluminum evaporated after the $\text{SiN}_{2.4}$. We find that these samples show extremely high series resistances of more than $10^5 \Omega \text{ cm}^2$ and thus verified that the $\text{SiN}_{n=2.4}$ acts as a barrier for the Al. We can therefore conclude that the contact occurs only in the highly-doped LTD regions, where the thin passivating $\text{SiN}_{n=2.4}$ layer has been removed and local heavy doping has been established via our LTD process. We take this finding as the basis for our assumption that the surface recombination velocity remains at the same low level (around 10 cm/s) in the passivated ($\text{SiN}_{n=2.4}$ -coated) region regardless of the absence or presence of Al on top.

The second structures are reference solar cells without LTD, and are labeled as “No-LTD”. In this case the aluminum is evaporated directly on top of the FSF and before the $\text{SiN}_{n=2.4}$, in order to establish a contact. We use the same grid as for the design “Crossed” and “Fine” with a metallization fraction of 3%.

2.2 Solar cell results

Figure 6 shows the cell parameters for the different LTD-metallization designs, including a reference without laser process. The legend shows additionally the metallization fraction that corresponds to the configurations of the cells (see Figure 4 b). Note that the actual semiconductor-metal contact area fraction is smaller than the total metallization fraction for the “Crossed” and “Fine” configuration. The data shows a strong dependence of the open-circuit voltage V_{oc} on the laser energy. V_{oc} reduces strongly from 673mV to 633mV upon increasing the laser power from 6 to 60 μJ . Also the short circuit current, J_{sc} exhibits a pronounced dependence on the LTD laser power. Both effects are due to the increased recombination as has been investigated and illustrated separately in Figure 2. As expected in solar cells with the junction at the rear side, this additional front side recombination contributes strongly to the reduction of the short circuit current, too. We therefore find that the LTD process either has to be performed with minimal laser power, or a more controlled (defect-free) re-crystallization of the laser-melted silicon needs to be established. The reference cell “No-LTD” and with a metallization fraction of 3% shows also reduced values of V_{oc} and J_{sc} . Specially detrimental is the reduction of the open circuit voltage below 530 mV. One reason for this degradation may be found in the strong recombination behavior of the thin transparent and passivated FSF, supported by the classical theory of recombination within emitter regions [11]. Additionally there could be spiking during evaporation of aluminum. Typically spiking produces local perforation of the thin FSF, thus exposing the interface between the wafer bulk and the FSF to high recombination sites.

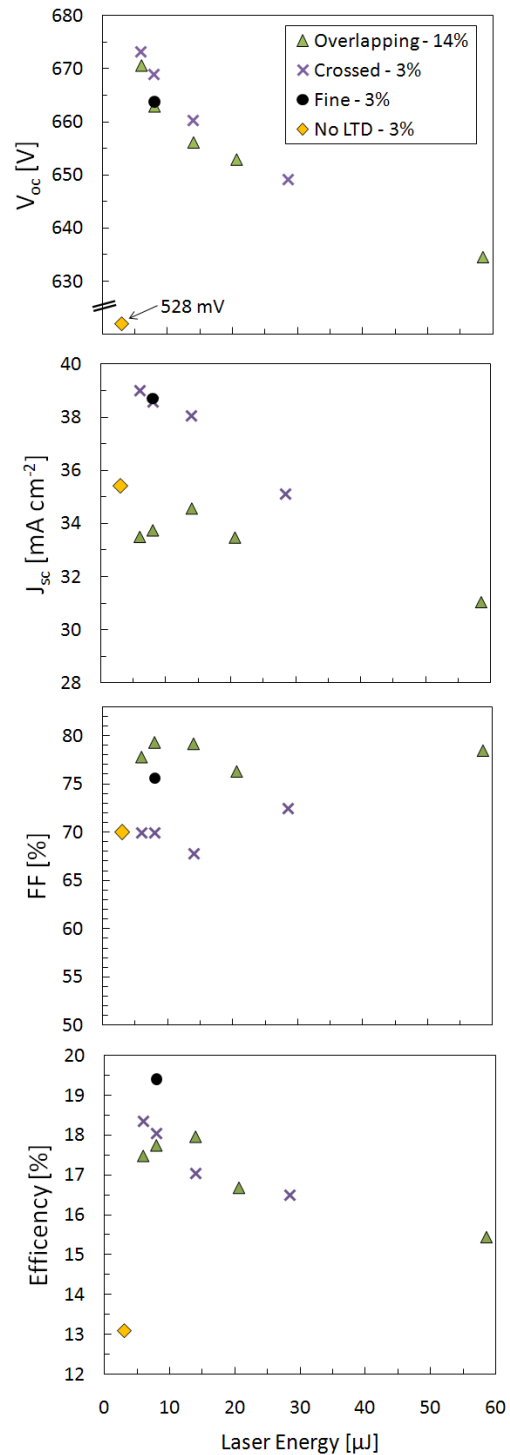


Figure 6: Cell parameters for back junction solar cells with selective front surface field produced by Laser Transfer Doping. A reference without LTD is also included, and in this case the Al is coated prior the deposition of the $\text{SiN}_{n=2.4}$.

Shading from the metallization needs to be taken into account when assessing the J_{sc} values. The designs “Crossed” and “Fine” have a metal coverage fraction of 3%. We find that for the same laser energy the J_{sc} values of the “fine” and of the “crossed” configuration lay consistently at the same level around 38.6 mA cm^{-2} . Taking in consideration additional shading up 14% for

the “overlapping” configuration gives a reduced values of $J_{sc} = 34.2 \text{ mA cm}^{-2}$. This reduction from considering shading only coincides reasonably with the J_{sc} value the cell with “Overlapping” design at the same laser power of the LTD process. Therefore, we can conclude that the difference in J_{sc} between the cells with the fine grid (“fine” and “crossed”, ~3% shading) and the coarse grid design (“overlapping”, with ~16% contact shading) is produced primarily by shading.

On the other hand, the fill factor, FF , is very sensitive to the design used and almost not influenced by the laser energy. In the “Overlapping” design it remains around 79% regardless the laser energy used. The other two designs, with a very small contact area, reduce the fill factor below 76%, but their values show a discrepancy with the corresponding contact areas. The best cell is for the “Fine” cell, with a contact area of 0.3%, is higher than the best measured for the “Crossed” configuration, with a contact area of 0.6%.

The efficiency follows the trend of the open circuit voltage and short circuit current. Table I sums up the most relevant solar cells results. All the LTD designs lead to a high improvement of the efficiency when compared with the reference without LTD. The best cell is for the “Fine” design and processed with at low laser energy, reaching an efficiency of 19.4%.

The equation $V_{oc} = V_{th} \ln(J_{sc}/J_0+1)$, provides an approximation to calculate the total saturation current densities of our solar cell. In case of the “crossed” cell with the lowest laser power, we find that this cell has a total J_0 of 220 fA cm^{-2} . According to our data in Figure 2, we may associate 190 fA cm^{-2} of this saturation density with the 14% LTD-treated surface area. This leaves only

30 fA cm^{-2} for the rest of the cell. However, the sum of the values for the passivated regions (23 fA cm^{-2}) and at the rear side (150 fA cm^{-2} as reported in [9]) exceeds this amount. A possible explanation could be the different geometries between the LTD pattern in lifetime references (homogeneously distributed points) and solar cells (densely packed rectangular pattern of LTD points). In any case, we see that the simplified approach of summing up the area weighted J_0 -values of the surfaces does not seem to yield a good approximation to the solar cell total saturation current density $J_{0,total}$ for our LTD-processed cells. The effect of the LTD process on the solar cell performance will be addressed in more detail in future investigations.

3 CONCLUSIONS

We demonstrate and characterize Laser Transfer Doping (LTD) by laser-transferring doped amorphous silicon onto silicon wafers. In our investigation here, we perform LTD through passivating dielectric layers in order to produce locally heavily doped regions with low contact resistance. The laser energy is the dominant parameter affecting both recombination at the contacts and contact resistance. Lowest laser powers values produce the lowest recombination, whilst higher energy values are preferred for minimizing contacts resistance. We use LTD to contact the front surface field of back junction solar cells and demonstrated in these initial experiments solar cell efficiencies of up to 19.4%.

Table I: Process and performance parameters for the most relevant solar cells

Cell	Laser Energy [μJ]	Design	Fraction			Voc [mV]	Jsc [mA cm^{-2}]	FF [%]	Eff. [%]
			Metal [%]	LTD [%]	Contact [%]				
Best FF	8	Overlapping	14	14	14	663	33.4	79.3	17.7
Best V_{oc} and J_{sc}	6	Crossed	3	14	0.6	673	39.0	69.91	18.4
Best cell	8	Fine	3	5	0.3	664	38.7	75.6	19.4
No LTD	0	No LTD	3	0	3	528	35.4	70.0	13.1

ACKNOWLEDGEMENTS

We acknowledge gratefully S.Mau for clean room processing and A. Schmidt for help in solar cell characterization. We also gratefully acknowledge the institutional funding of ISFH by the State of Lower Saxony.

REFERENCES

- [1] D. Kray and S. Glunz, Prog. Photovolt: Res. Appl. **14**, 195 (2006)
- [2] D.Suwito, U. Jäger, J. Benick, S. Janz, M. Hermle, R. Preu, S.W. Glunz, Proceedings of the 25th European Photovoltaic Conference, Valencia, Spain, 2010, pp. 1443-1445
- [3] P. Mei, J.B. Boyce, J.P. Lu, J. Ho, and R.T. Fulks, J. Non-Cryst. Solids **266**, 1252 (2000).
- [4] P. Mei, R.A. Lujan, J.B. Boyce, US patent 5 871 826, 1999.
- [5] R. Ferré, R. Gogolin, J. Müller, N.P. Harder, and R. Brendel, pssa (2011), DOI 10.1002/pssa.201127046
- [6] J. Mueller, K. Bothe, S. Gatz, F. Haase, C. Mader and R. Brendel, Journal of Applied Physics **108**, 124513 (2010)
- [7] B. Fischer, Loss analysis of crystalline silicon solar cells using photoconductance and quantum efficiency measurements, Ph.D. thesis, University Konstanz, 2003
- [8] R. Brooks, and H. Mattes, Bell Systems Technical Journal 1971, **50** pp. 775–785.
- [9] M. Kessler, D. Münster, T. Neubert, C. Mader, J. Schmidt, R. Brendel, Proc 37th PVSC-IEEE Conference, June 2011, Seattle
- [10] L. Mai, S. R. Wenham, B. Tjahjono, J. Ji, and Z. Shi, Proc. IEEE 4th WCPEC, Waikoloa, Hawaii, May 7-12, 2006, p. 890
- [11] L. M. Castañer, P. Ashburn, L. Prat, and G. R. Wolstenholme, IEEE Trans. Electron Dev. **35**, 1902 (1988)